Supplementary Information

Impact of Molecular Symmetry on Single-Molecule Conductance

Emma J. Dell,[1,§] Brian Capozzi,[2,§] Kateri H. DuBay,[1] Timothy C. Berkelbach,[1] Jose Ricardo Moreno,[1] David R. Reichman,[1] Latha Venkataraman,*[,2] Luis M. Campos.*[,1]

[1]Department of Chemistry and [2]Department of Applied Physics and Applied Mathematics, Columbia University, New York, NY 10027, USA.

[§] These authors contributed equally to this study.

Author e-mail address: lv2117@columbia.edu; lcampos@columbia.edu

Contents:

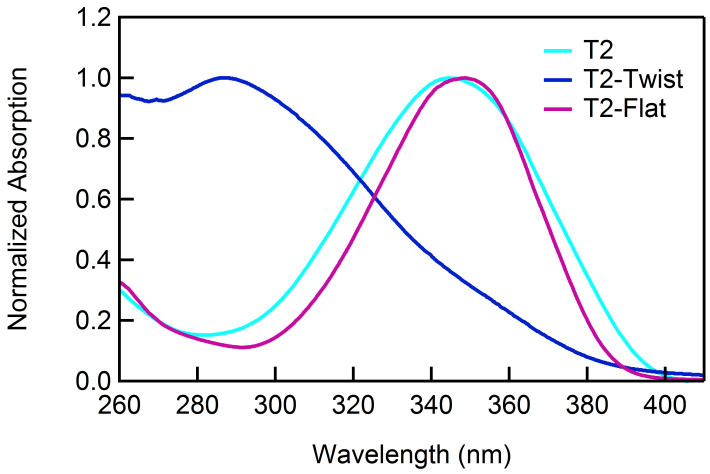

Figure S1: UV-vis absorption data taken in DCM for T2, T2-flat and T2-twist.

Synthesis Details:

All reactions were performed in oven-dried round bottom flasks, unless otherwise noted. The flasks were fitted with rubber septa and reactions were conducted under a positive pressure of argon, unless otherwise noted. Anhydrous solvents were obtained from a Schlenk manifold with purification columns packed with activated alumina and supported copper catalyst (Glass Contour, Irvine, CA). Stainless steel syringes or cannulae were used to transfer air- and moisture-sensitive liquids. Flash column chromatography was performed employing 32-63 μm silica gel (Dynamic Adsorbents Inc). Thin- layer chromatography (TLC) was performed on silica gel 60 F_{254} plates (EMD).

*Materials***.** Commercial reagents were used without further purification with the exception of N-bromosuccinimide which was recrystallized from hot water. Commercial reagents purchased from Sigma Aldrich include *n*-butyllithium (2.5M in hexanes), potassium carbonate, 5,5'-dibromo-2,2'-bithiophene, 2,2'-bithiophene, 2,2':5',2''-terthiophene, thiophene, 3-hexylthiophene, N-bromosuccinimide, 2-Isopropoxy-4,4,5,5-tetramethyl-1,3,2-dioxaborolane, triethylamine, 4,4'-bis-methylsulfanyl-biphenyl. Commercial reagents purchased from Strem Chemicals include Tetrakis(triphenylphosphine) palladium(0). Commercial reagents purchased from Acros Organics include tributyltin chloride, 2,5-dibromothiophene, dimethyl disulfide, 3,4-dibromothiophene, n-hexyl magnesium bromide. Commercial reagents purchased from Lumtec include 2,6-Dibromo-4H-cyclopenta[2,1-b:3,4-b']dithiophene.

*Instrumentation***.** Proton nuclear magnetic resonance (^{1}H NMR) spectra and carbon nuclear magnetic resonance (^{13}C NMR) spectra were recorded on a Bruker DRX300 (300 MHz) and a Bruker DRX400 (400 MHz) spectrometer. Chemical shifts for protons are reported in parts per million downfield from tetramethylsilane and are referenced to residual protium in the NMR solvent ($CHCl_3$: d 7.26). Chemical shifts for carbon are reported in parts per million downfield from tetramethylsilane and referenced to the carbon resonances of the solvent ($CDCl_3$: d 77.0). Data are represented as follows: chemical shift, multiplicity (app = apparent, br = broad, s = singlet, d = doublet, t = triplet, q = quartet, m = multiplet), coupling constants in Hertz (Hz), and

integration. The mass spectroscopic data were obtained at the Columbia University mass spectrometry facility using a JEOL JMSHX110A/110A tandem mass spectrometer. Absorption spectra were taken on a Shimadzu UV-1800 spectrophotometer.

1. 5,5'-bisthiomethyl 2,2'-bithiophene **(T2)**

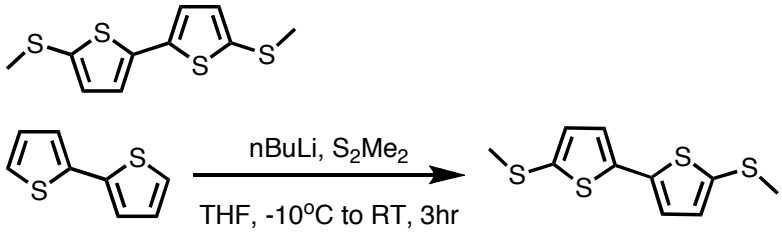

An oven-dried 50 mL round bottom flask and stir bar were cooled under Ar. 2,2'-Bithiophene was added (500 mg, 3.01 mmol, 1 eq) and dissolved in 20 ml THF. The flask was cooled to -10 ^{o}C. *n*-Butyllithium (2.5M in hexanes, 2.4 mL, 6.01 mmol, 2 eq) was added dropwise by syringe. The solution turned turquoise. The reaction was stirred at - 10 ^{o}C for 1 hour. Dimethyl disulfide (0.53 mL, 6.01 mmol, 2 eq) was added dropwise by syringe. The solution turned a milky yellow. The reaction was stirred at -10 ^{o}C for 30 minutes and then allowed to warm to room temperature and stirred for another 2 hours. The reaction was quenched with water. The biphasic mixture was poured into a separatory funnel and the organic and aqueous layers were separated. The aqueous layer was extracted two times with diethyl ether (2 x 25 mL) and the combined organic layers were washed with water (30 mL) and brine (30 mL) and dried over magnesium sulfate. After filtration, the organic layer was concentrated under reduced pressure. Purification by column chromatography in 100% hexanes (R_f = 0.17) yielded the product as a pale yellow solid (460 mg, 60% yield). ^{1}H NMR (400 MHz, $CDCl_3$) d 6.96 (s, 4H), 2.51 (s, 6H). ^{13}C NMR (400 MHz, $CDCl_3$) d 131.86, 123.94, 22.24. HRMS (FAB+) calculated for $C_{10}H_{10}S_4$ 258.45, found 258.78.

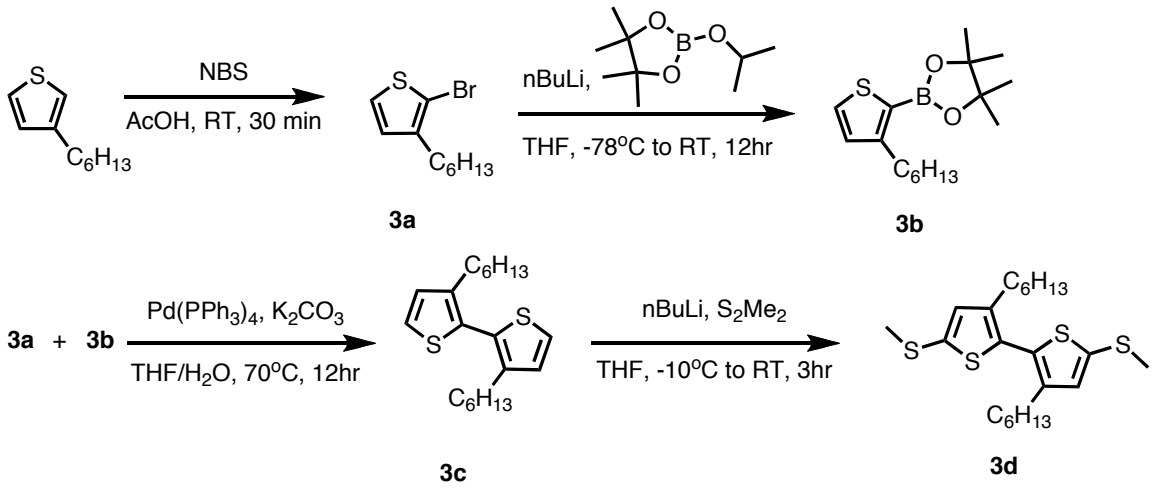

3a. 2-bromo,3-hexyl thiophene

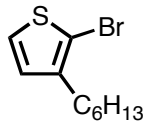

An oven-dried 50 mL round bottom flask and stir bar were cooled under Ar. 3-hexylthiophene (3 g, 17.8 mmol, 1 eq) was added and dissolved in 45 ml of acetic acid. N-bromosuccinimide (3.17 g, 17.8 mmol, 1 eq) was added and the solution was stirred for 30 minutes in the dark at room temperature. 45 mL of water was added and then the organic layer was extracted with diethyl ether (2 x 50 mL), washed with sodium hydrogen carbonate (2 x 50 mL), water (2 x 50 mL) and brine (50 mL) and dried over magnesium sulfate. After filtration, the organic layer was concentrated under reduced pressure to yield a colourless oil (4.15 g, 94%). This crude product was used in the next stage without further purification. ^{1}H NMR (400 MHz, $CDCl_3$) δ 7.19 (d, J = 5.6 Hz, 1H), 6.81 (d, J = 5.6 Hz, 1H), 2.58 (t, J = 7.7 Hz, 2H), 1.62-1.56 (m, 2H), 1.36-1.30 (m, 6H), 0.94-0.90 (t, 3H). ^{13}C NMR (400 MHz, $CDCl_3$) δ 142.09, 128.35, 125.24,108.93, 31.77, 29.85, 29.54, 29.04, 22.75, 14.23. LRMS (ESI+) calculated for $C_{10}H_{15}BrS$ 247.20, found 246.01.

3b. 3-hexyl thiophene-2-boronic acid pinacol ester

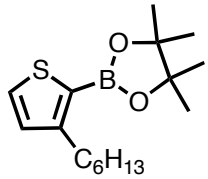

An oven-dried 100 mL round bottom flask and stir bar were cooled under Ar. **3a** (3 g, 12 mmol, 1 eq) was added and dissolved in 40 mL THF. The solution was cooled to -78 ^{o}C. *n*-Butyllithium (2.5M in hexanes, 5.5 mL, 13 mmol, 1.1 eq) was added dropwise by syringe and the solution was stirred for 30 minutes at -78 ^{o}C.

2-Isopropoxy-4,4,5,5-tetramethyl-1,3,2-dioxaborolane (2.48 g, 13 mmol, 1.1 eq) was added dropwise by syringe. The solution was allowed to warm to room temperature and stirred overnight. The reaction was quenched by adding 30 mL of water. The organic layer was extracted with diethyl ether (2 x 40 mL), washed with water (50 mL) and brine (50 mL) and dried over magnesium sulfate. After filtration, the organic layer was concentrated under reduced pressure to yield a yellow oil (3.3 g, 92% yield). This crude product was used in the next stage without further purification. ^{1}H NMR (400 MHz, $CDCl_3$) δ 7.47 (d, J = 4.6 Hz, 1H), 7.01 (d, J = 4.7 Hz, 1H), 2.89 (t, J = 7.7 Hz, 2H), 1.65-1.57 (m, 2H), 1.33 (s, 12H), 1.29 (m, 6H), 0.91-0.89 (t, 3H). ^{13}C NMR (101 MHz, $CDCl_3$) δ 154.83, 148.34, 131.39, 130.42, 83.65, 31.91, 31.81, 30.26, 29.11, 24.93, 22.76, 14.26. LRMS (APCI+) calculated for $C_{16}H_{27}BO_2S$ 294.26, found 294.23.

3c. 3,3'dihexyl, 2,2' bithiophene

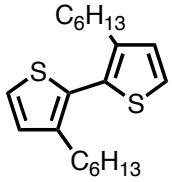

An oven-dried 2 necked 50 mL round bottom flask and stir bar were fitted with a condenser and cooled under Ar. **3a** (200 mg, 0.81 mmol, 1 eq) was added and dissolved in 5 mL of THF that had been sparged with Ar for 20 minutes. Potassium carbonate (112 mg, 0.81 mmol, 1 eq) dissolved in 5 mL of water that had been sparged with Ar for 20 minutes was added by cannula. Tetrakis(triphenylphosphine) palladium(0) (94 mg, 0.081 mmol, 0.1 eq) was added and the solution was heated to 70 ^{o}C. **3b** (238 mg, 0.81 mmol, 1 eq) was added dropwise and the solution was refluxed at 70 ^{o}C overnight. The solution was allowed to cool and then the organic layer was extracted with $CHCl_3$ (2 x 15 mL) and washed with water (20 mL) and brine (20 mL) and dried over magnesium sulfate. After filtration, the organic layer was concentrated under reduced pressure. Purification by column chromatography in 100% hexanes (R_f = 0.39) yielded

the product as a yellow oil (260 mg, 96% yield). ^{1}H NMR (400 MHz, $CDCl_3$) δ 7.29 (d, J = 5.3 Hz, 2H), 6.97 (d, J = 5.2 Hz, 2H), 2.53 (t, 4H), 1.58-1.55 (m, 4H), 1.29-1.25 (m, 12H), 0.92-0.88 (t, 6H). ^{13}C NMR (101 MHz, $CDCl_3$) δ 14.0, 22.6, 28.8, 29.1, 30.7, 31.6, 125.2, 128.5, 128.7, 142.3 LRMS (APCI+) calculated for $C_{20}H_{30}S_2$ 334.58, found 334.11.

3d. 5,5' bisthiomethyl, 3,3'dimethyl, 2,2' bithiophene **(T2-twist)**

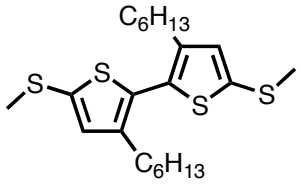

The title compound was prepared on a 0.30 mmol scale according to the procedure for compound **2** with the following modification: **3c** (100 mg, 0.30 mmol) was used instead of 2,2'-bithiophene. Purification by column chromatography in 100% hexanes (R_f = 0.16) yielded the product as a yellow oil (59 mg, 46% yield). ^{1}H NMR (400 MHz, $CDCl_3$) d 6.89 (s, 2H), 2.51 (s, 6H), 2.42 (t, 4H), 1.52 (m, 4H), 1.21 (m, 12H), 0.86 (t, 6H). ^{13}C NMR (400 MHz, $CDCl_3$) δ 143.11, 137.09, 131.83, 130.29, 31.75, 30.71, 29.21, 29.03, 22.71, 21.66, 14.22. LRMS (APCI+) calculated for $C_{22}H_{34}S_4$ 426.77, found 425.82.

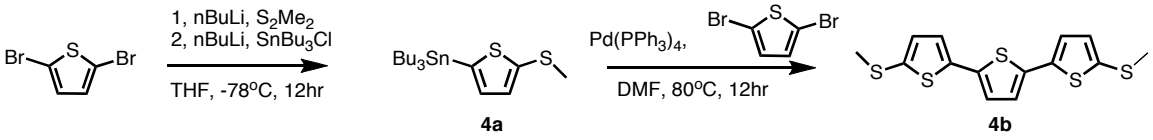

4, 2,6-Dithiomethyl-4H-cyclopenta[2,1-b:3,4-b']dithiophene **(T2-Flat)**

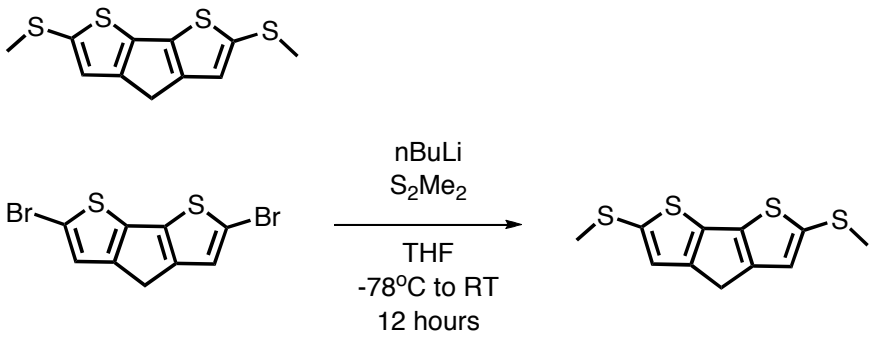

An oven-dried 25 mL round bottom flask and stir bar were cooled under Ar. 2,6-Dibromo-4H-cyclopenta[2,1-b:3,4-b']dithiophene (100 mg, 0.29 mmol, 1 eq) was added and dissolved in 7 mL THF. The solution was cooled to -78 ^{o}C. *n*-Butyllithium (1M in hexanes, 0.60 mL, 0.59 mmol, 2 eq) was added dropwise by syringe and the solution was stirred for 10 minutes at -78 ^{o}C. The solution turned yellow upon addition of *n*-butyllithium. Dimethyl disulfide (56 mg, 0.59 mmol, 2 eq) was added dropwise by syringe and the solution turned a brighter yellow. The solution was allowed to warm to room temperature and stirred overnight. The solution was washed with water (2 x 20ml), dried over magnesium sulfate. After filtration, the organic layer was concentrated under reduced pressure. Purification by column chromatography in 100% hexanes (R_f = 0.23) yielded the product as a pale orange powder (20 mg, 25% yield). ^{1}H NMR (400 MHz, $CDCl_3$) d 7.14 (s, 2H), 3.48 (s, 2H), 2.50 (s, 6H). ^{13}C NMR (400 MHz, $CDCl_3$) δ 148.53, 141.34, 136.65, 128.79, 32.48, 23.33. HRMS (ESI+) calculated for $C_{11}H_{10}S_4$ 270.46, found 270.08.

Theoretical Details:

Potential Energy Curves

The inter-ring dihedral angle potential energy curves shown in Figure 3 were calculated using the OPLS-SB-T force field, a version of OPLS-2005 that has been optimized for conjugated polymers,[1] within MacroModel.[2] These curves were calculated in a few different ways, as described in the main text, to probe the effect of restricting the distance between the two gold-binding sites on the potential energy surface of the molecule's inter-ring torsion. We were interested in elucidating the difference due to the pedaling motion that is involved in rotations of the bithiophene inter-ring torsion (see Figure 2E). It is important to note that Figure 3 presents the relative energy curves, and thus all the curves have a zero relative energy value at some value of θ. This feature explains, for example, the discrepancy between the solid curve and the long dashed curve in Figure 3B at low θ-values.

MD Simulations

The molecular dynamics simulations were run using DESMOND[3,4] and OPLS-SB-T.[1] Each simulation consisted of a single molecule in a vacuum. Sampling was done within the NVT ensemble at 300K, utilizing a Nose-Hoover thermostat. No cutoffs were implemented. For all four of the molecules considered here, two sets of MD simulations were run: (1) The atoms in the initial simulations were completely unrestricted. This 51 ns simulation was allowed to equilibrate for 1 ns and then starting configurations for the next set of simulations were collected every 100 ps, provided a total of 500 sample configurations that might be expected to "jump" into the junction. (2) The next set of MD simulations consisted of 500 runs, each with a different starting configuration taken from the first set of simulations. The distance between the Au-attaching sulfur atoms was then restricted, and MD simulations were run for 2 ns. Again, the molecule was allowed to equilibrate for the first ns, and then the position of θ was recorded every 2 ps during the second ns, yielding 500 θ-values for each of the 500 different "bound" runs. No attempt is made to replicate the effects of pulling, and we note that, on the timescale of a single conductance data point measurement (~25 microseconds), the distance between the electrodes should only change by approximately 0.005 Angstroms, as the pulling rate in the experiment is 20nm/s.

Torsion Angle Fluctuations in Time.

In the unrestricted simulations, the biphenyl and bithiophene molecules explore most of the available configurational θ space, whereas the T2-twist and T2-flat molecules access only a small region of the θ state space. When the distance between the Au-attaching sulfur atoms is restricted, the simulations of biphenyl, T2-twist, and T2-flat again access approximately the same region of θ state space as in the unrestricted simulations (although the barriers in biphenyl appear to slow the molecule's exploration of θ state space, such that there are correlations in the θ–values on the sampling timescale, which is still far shorter than the measurement timescale). Bithiophene, however, behaves differently, and the θ-values in the different "bound" runs segregate into different regions of θ state space, remaining there for the entire 2 ns of simulation time. This trend reflects the alterations observed in the potential energy curve upon freezing the positions of the Au-attaching atoms (see Figure 3B). The difference this makes in terms of the distributions of torsion angles sampled during a single restricted trace can be seen in Figure 3E-H, where the distribution of the inter-ring torsion angle is plotted for the first ten restricted MD simulations. The fact that the distribution curves shown for biphenyl are nearly identical between different runs whereas those for bithiophene vary substantially illustrates the difference between these two molecules in terms of the different effect junction binding has on the resulting distributions of inter-ring torsion angles sampled within a given "junction-bound" state.

Conductance proportional to $\cos^2\theta$. Single molecule conductance, G, is assumed proportional to the square of the electronic coupling matrix element, or charge-transfer integral, t. For molecules with torsional degrees of freedom, the transfer integral is typically assumed to follow a cosine dependence, $t \sim \cos(\theta)$, yielding a conductance that is proportional to $\cos^2(\theta)$. The accuracy of this $\cos^2(\theta)$ law has been previously demonstrated in a system of biphenyl derivatives.[5] To confirm that this $\cos^2(\theta)$ dependence of the conductance also holds for thiophenes, we have performed electronic structure calculations using the GAMESS quantum chemistry package.[6] The charge-transfer integral, $t(\theta)$, was estimated from the energy splitting of the highest occupied molecular orbitals (HOMOs), corresponding to hole transport: $2t$ =

E(HOMO)-E(HOMO-1). Calculations were performed with density functional theory and the PBE exchange-correlation functional,[7] with a 6-31G(d) basis set. S-H end groups were employed as a simpler substitute for the experimental S-CH_3 groups. The geometry was optimized at the planar, θ=0°, configuration, and then rotated about the torsional angle in 10° increments without additional optimization. The results for biphenyl and bithiophene, shown in Figure S2 confirm that the charge-transfer integral follows a cos(θ) dependence to an excellent degree of accuracy; similar results have previously been found for P3HT.[8] These results confirm that the experimental conductance histogram can be qualitatively modeled by the statistical properties of $\cos^2(\theta)$ obtained from MD simulations, described below.

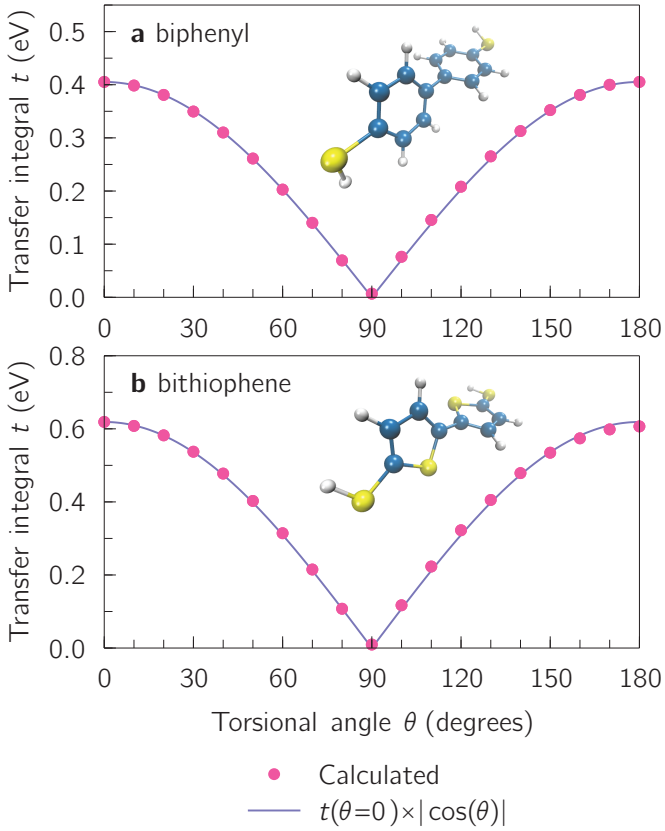

Figure S2. Charge-transfer integral corresponding to hole transport through biphenyl (a) and bithiophene (b) as a function of the inter-ring torsional angle, confirming the predicted cos(θ) dependence.

Variations in $\cos^2(\theta)$. To further characterize the dynamic behavior of these molecules and estimate their effects on conductance, for each q −value observed during the "bound" part of the MD simulations described above, we also calculated the value of $\cos^2(\theta)$. Average values of $\cos^2(\theta)$ were then calculated for each of the 500 "bound" runs (the average $\cos^2(\theta)$ value represents, proportionally, a single conductance measurement for that run, as the timescale of the true conductance experiments far exceeds the simulation timescale). Finally, the averages and standard deviations of the single-run-averaged $\cos^2(\theta)$ values were calculated between the 500 differently-"bound" runs. Results are shown in Table S1. They again reflect the trends observed above for the individual trajectories. The T2-twist and T2-flat molecules have the most consistent average $\cos^2(\theta)$ values across the 500 different "bound" simulations, reflecting the relatively small effect of fixing the Au-attachment points on their potential energy curves (see Figure 3). Biphenyl explores four different θ angle energy basis, and it appears to move between these on a timescale that is not negligible when compared to the simulation length, however the energy basins all have approximately the same value of $\cos^2(\theta)$, and thus the standard deviation in this value observed across the 500 runs for this value is relatively small. Bithiophene, on the other hand, fluctuates within altered energy wells that depend on the configuration of the fixed Au-attached sulfurs. The $\cos^2(\theta)$ values reflect the variations in the energy potential of the differently-bound configurations, and a large standard deviation is observed between the 500 different "bound" runs.

Table S1: Averages and standard deviations of $\cos^2(\theta)$ between different "bound" MD simulations.

Molecule	$\cos^2(\theta)$
biphenyl	0.439 ± 0.062
bithiophene	0.621 ± 0.132
T2-twist	0.090 ± 0.031
T2-flat	0.959 ± 0.004

References:

(1) DuBay, K. H.; Hall, M. L.; Hughes, T. F.; Wu, C.; Reichman, D. R.; Friesner, R. A. *J Chem Theory Comput*, **2012**, DOI: 10.1021/ct300175w

(2) MacroModel User Manual. Schrodinger, LLC: New York, NY. **2008**.

(3) Desmond Molecular Dynamics System, version 3.0, D. E. Shaw Research, New York, NY, 2011. Maestro-Desmond Interoperability Tools, version 3.0, Schrödinger, New York, NY, **2011**.

(4) Bowers, K. J.; Chow, E.; Xu, H.; Dror, R. O.; Eastwood, M. P.; Gregersen, B. A.; Klepeis, J. L.; Kolossvary, I.; Moraes, M. A.; Sacerdoti, F. D.; Salmon, J. K.; Shan, Y.; Shaw, D. E. *Proceedings of the ACM/IEEE Conference on Supercomputing*, Tampa, Florida, November 11-17, **2006**.

(5) Venkataraman, L.; Klare, J. E.; Nuckolls, C.; Hybertsen, M. S.; Steigerwald, M. L. *Nature* **2006**, *442*, 904.

(6) Schmidt, M. W.; Baldridge, K. K.; Boatz, J. A.; Elbert, S. T.; Gordon, M. S.; Jensen, J. H.; Koseki, S.; Matsunaga, N.; Nguyen, K. A.; Su, S.; Windus, T. L.; Dupuis, M.; Montgomery, J. A. *J Comput Chem* **1993**, *14*, 1347

(7) Perdew, J. P.; Burke, K.; Ernzerhof, M. *Phys. Rev. Lett.* **1996**, *77*, 3865.

(8) Grozema, F. C.; van Duijnen, P. Th.; Berlin, Y. A.; Ratner, M. A.; Siebbeles, L. D. A. *J. Phys. Chem. B* **2002**, *106*, 7791